

Enantiomeric Inclusion of α -Hydroxy Esters by (*R*)-(1-Naphthyl)glycyl-(*R*)-phenylglycine and the Crystal Structures of the Inclusion Cavities

Motohiro Akazome, Toshiaki Takahashi,[†] and Katsuyuki Ogura*

Department of Materials Technology, Faculty of Engineering and Graduate School of Science and Technology, Chiba University, 1-33 Yayoicho, Inageku, Chiba 263-8522, Japan

Received September 15, 1998

A simple dipeptide, (*R*)-(1-naphthyl)glycyl-(*R*)-phenylglycine [(*R,R*)-**1**], formed inclusion compounds with several α -hydroxy esters (**2**) with high enantioselectivity. By crystallization of a mixture of the dipeptide [(*R,R*)-**1**] and racemic **2a** [MeCH(OH)COOMe] from methanol, asymmetric recognition occurred to give an inclusion compound that contains the *S* form of **2a** in 89% ee. X-ray crystallographic study of the inclusion compound elucidated that the dipeptide molecules arrange in a “folded antiparallel” β -sheetlike structure to accommodate the α -hydroxy ester in the pocket-type cavity surrounded by naphthyl and phenyl groups on the sheet. Similarly, **2b** [MeCH(OH)COOEt] and **2f** [dihydro-3-hydroxy-4,4-dimethyl-2(3*H*)-furanone] were included with high enantioselectivity of the *S* form. When bulkier **2i** [*t*-BuCH(OH)COOMe] was used as a guest molecule, the arrangement of dipeptide molecules changed to an “extended antiparallel” mode, where the naphthyl and phenyl groups arranged in a “parallel stacked and displaced” mode and a channel-type cavity was constructed. The guest molecules were accommodated via hydrogen bonding in the channel-type cavity with high enantioselectivity of the *S* form (82% ee). In the case of **2k** [*i*-PrCH(OH)COOMe], optically pure (*S*)-**2k** formed the dipeptide sheet with the “folded antiparallel” structure by cocrystallization with (*R,R*)-**1**, while the “extended antiparallel” structure appeared in the inclusion of racemic **2k**.

Introduction

Crystal engineering to control crystal packing is an exciting field in science.¹ The molecules are arranged regularly in crystals through intermolecular interaction such as hydrogen bonding, ionic pairing, coordinate bonding, and hydrophobic interaction. When crystalline host molecules self-assemble through noncovalent bonding, guest molecules are often included in their crystal lattice.^{2,3}

Our attention has been paid to dipeptide molecules, which have a relatively straight structure because its central amide group scarcely rotates. Many dipeptide molecules are known to self-assemble into various sheet structures.⁴ We have reported that (*R*)-arylglycyl-(*R*)-phenylglycine (aryl = phenyl or naphthyl) constructs a channel-type or pocket-type cavity for inclusion of guest

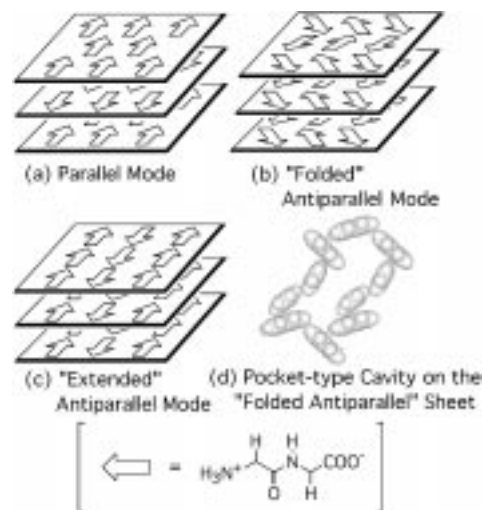


Figure 1. (a–c) Schematic drawings of three hydrogen-bonding sheets of (*R,R*)-**1** backbones. (d) A pocket-type cavity that included guest molecules.

molecules, which is constructed by naphthyl and phenyl groups placed perpendicular to the sheet.⁵ Crystalline (*R*)-(1-naphthyl)glycyl-(*R*)-phenylglycine [(*R,R*)-**1**] molecules form two types of β -sheetlike arrangement by hydrogen bonding (a and b in Figure 1). According to the kind of guest molecule, ether or alcohol, (*R,R*)-**1** molecules form a “parallel” or “antiparallel” β -sheetlike structure, respectively;⁶ the “parallel” mode has a channel-type

[†] Graduate School of Science and Technology.

(1) Recent review on inclusion compounds. *Comprehensive Supramolecular Chemistry, Volume 6, Solid-state Supramolecular Chemistry: Crystal Engineering*; MacNicol, D. D., Toda, F., Bishop R., Eds.; Pergamon Press: Oxford, 1996.

(2) *Molecular Inclusion and Molecular Recognition—Clathrates I and II*; Weber, E., Ed.; Springer-Verlag: Berlin and Heidelberg, 1987 and 1988; Vols. 140 and 149.

(3) (a) Aoyama, Y.; Endo, K.; Kobayashi, K.; Masuda, H. *Supramolecular Chem.* **1995**, *4*, 229. (b) Kolotuchin, S. V.; Fenlon, E. E.; Wilson, S. R.; Loweth, C. J.; Zimmerman, S. C. *Angew. Chem., Int. Ed. Engl.* **1995**, *34*, 2654. (c) Su, D.; Wang, X.; Simard, M.; Wuest, J. D. *Supramolecular Chem.* **1995**, *66*, 171. (d) Ung, A. T.; Gizachew, D.; Bishop, R.; Cance, M. L.; Craig, D. C. *J. Am. Chem. Soc.* **1995**, *117*, 8745. (e) Endo, K.; Koike, T.; Soak, T.; Hayashida, O.; Masuda, H.; Aoyama, Y. *J. Am. Chem. Soc.* **1997**, *119*, 4117. (f) Brunet, P.; Simard, M.; Wuest, J. D. *J. Am. Chem. Soc.* **1997**, *119*, 2737. (g) Suzuki, H.; Takagi, H.; Sato, R. *Tetrahedron Lett.* **1997**, *38*, 4563.

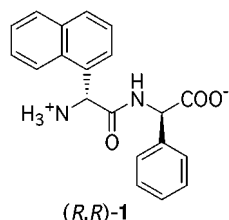
(4) (a) Görbitz, C. H.; Etter, M. C. *Int. J. Protein Res.* **1992**, *39*, 93. (b) Suresh, C. G.; Vijayan, M. *Int. J. Protein Res.* **1985**, *26*, 311. (c) Ashida, T.; Tanaka, I.; Yamane, Y. *Int. J. Protein Res.* **1981**, *17*, 322.

(5) Akazome, M.; Yanagita, Y.; Sonobe, R.; Ogura, K. *Bull. Chem. Soc. Jpn.* **1997**, *70*, 2823.

(6) Akazome, M.; Sumikawa, A.; Sonobe, R.; Ogura, K. *Chem. Lett.* **1996**, 995.

cavity,⁵ and a pocket-type cavity surrounded by naphthyl and phenyl groups appears in the “antiparallel” mode as shown in Figure 1d.

Since the pocket-type cavity in the antiparallel mode of (*R,R*)-(1-naphthyl)glycyl-(*R*)-phenylglycine is chiral, we initiated our investigation on its asymmetric recognition for chiral guests. As a result, we found that α -hydroxy esters,⁷ which have two functional groups to make synergistic hydrogen bonding (vide infra), were included tightly in this chiral pocket-type cavity. Herein we report that (*R,R*)-**1** recognized α -hydroxy esters with high enantioselectivity and host–guest interactions were elucidated by single-crystal X-ray analysis. In addition, we found that some inclusion compounds exhibit a new “extended antiparallel” mode with a channel-type cavity, which is the third arrangement of (*R,R*)-**1** molecules (Figure 1c).



Results and Discussion

Inclusion Compounds of (*S*)-Methyl Lactate and Its Derivatives: “Folded Antiparallel” Mode of Dipeptide with a Pocket Cavity. Inclusion compounds were prepared by cocrystallization from a methanolic solution of (*R,R*)-**1** and racemic α -hydroxy esters (2 molar equiv). Using racemic methyl lactate (**2a**) as the guest molecule, (*R,R*)-**1** and **2a** molecules cocrystallized to form an inclusion compound [(*R,R*)-**1**:**2a** = 1:1] with high enantioselectivity [89% ee (*S*)] for **2a**. Single crystals of the inclusion compound suitable for X-ray crystallography were obtained by crystallization of (*R,R*)-**1** with optically pure (*S*)-**2a** (see Table 2). Figures 2–4 show selected drawings based on its crystal structure. The salt formation between the amino group and the carboxyl group of (*R,R*)-**1** and the hydrogen bonding network construct a sheet structure (Figure 2).

The salt formation between the amino group and the carboxyl group of (*R,R*)-**1** contributes the linkage along the *a* axis ($N^1 \cdots O^{*1}$ and $N^{*3} \cdots O^3$, 2.66 and 2.70 Å, respectively) to form a one-dimensional ribbon structure. The central amide hydrogen of (*R,R*)-**1** is bound to the terminal carboxylate of the neighboring (*R,R*)-**1** molecule with 2.93 ($N^{*2} \cdots O^{*4}$) and 2.83 ($N^{*4} \cdots O^{*2}$) Å, and the amide oxygen is bound to a terminal amino group of the opposite neighboring (*R,R*)-**1** molecule with 2.89 ($N^1 \cdots O^5$) and 2.93 ($N^3 \cdots O^6$) Å to construct the linkage along the *c* axis. These hydrogen bonds combine adjacent ribbons to construct a two-dimensional sheet, the mode of which we call “folded antiparallel” (Figure 1b). This “folded antiparallel” mode on the arrangement of (*R,R*)-**1** dipeptide backbones is closely similar to the inclusion

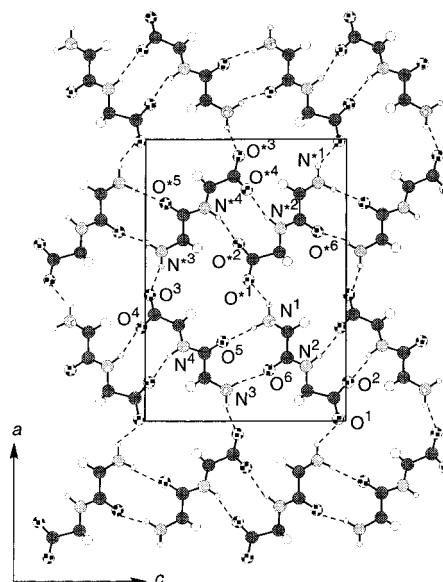


Figure 2. Sheet structure of dipeptide backbones of the inclusion compound (*R,R*)-**1**·(*S*)-**2a** (the *a*–*c* plane). The naphthyl and phenyl groups of (*R,R*)-**1** and (*S*)-**2a** are omitted for clarity. A unit cell is shown using a box.

compound of an allylic alcohol and (*R,R*)-**1**.⁶ Figure 3 shows crucial interactions between the guest molecules and the dipeptide backbone. An ammonio hydrogen of (*R,R*)-**1** was linked to one molecule (**A**) of **2a** via three-center hydrogen bonding⁸ ($N^1 \cdots O^{G1}$ and $N^1 \cdots O^{G2}$, 2.96 and 2.97 Å, respectively), and the hydroxyl group of **2a** was also bound to COO^- of (*R,R*)-**1** ($O^3 \cdots O^{G1}$, 2.76 Å). Another molecule (**B**) of **2a** was bound to $^+NH_3$ at the carbonyl group ($N^3 \cdots O^{G3}$, 2.80 Å) and to COO^- of the neighboring dipeptide at the hydroxyl group ($O^1 \cdots O^{G4}$, 2.80 Å). These multiple hydrogen bonds gave rise to tight inclusion and restricted conformation of the guest molecule, which contributed to stereospecific interaction on hydrophobic regions of the chiral cavity.

Hydrophobic interactions between aryl groups of (*R,R*)-**1** and the guest are shown in Figure 4: (*R,R*)-**1** molecules construct chiral pocket-type cavities surrounded by naphthyl and phenyl groups, and two (*S*)-**2a** molecules are included in one chiral cavity. In addition, hydrophobic interaction such as CH/π interaction⁹ was observed between the aryl groups of (*R,R*)-**1** and the alkyl groups of (*S*)-**2a** to assist the stabilization of the inclusion compound. This highly enantiomeric inclusion of (*S*)-**2a** prompted us to examine the inclusion of several α -hydroxy esters by (*R,R*)-**1** crystals.

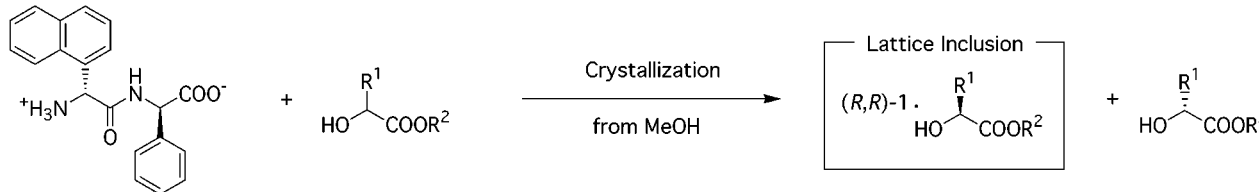
The results are summarized in Table 1. Methyl lactate (**2a**) and ethyl lactate (**2b**) afforded the corresponding 1:1 inclusion compounds with 89% ee (*S*) and 97% ee (*S*), respectively (entries 1 and 2). However, *n*-propyl lactate (**2c**) and isopropyl lactate (**2d**) were not included at all by (*R,R*)-**1** crystals (entries 3 and 4).

Methyl esters of other α -hydroxy carboxylic acids (**2e**, **2g**, **2h**, **2i**, and **2l**) except for **2k** were recognized in 87% ee (*S*), 89% ee (*S*), >99% ee (*S*), 87% ee (*S*), and 82% ee (*S*), respectively (entries 5, 7–9, 12, and 14). In a cyclic hydroxy ester, pantolactone **2f** was included in 92% ee (*S*) (entry 6).

(7) There are a few reports for enantiomeric inclusion of hydroxy esters by other crystalline hosts, see: (a) Cramer, F.; Dietsche, W. *Chem. Ber.* **1959**, *92*, 378. (b) Toda, F.; Tohi, Y. *J. Chem. Soc., Chem. Commun.* **1993**, 1238. (c) Toda, F.; Tanaka, K. *Tetrahedron Lett.* **1988**, *29*, 1807. (d) Toda, F.; Sato, A.; Tanaka, K.; Mak, T. C. W. *Chem. Lett.* **1988**, 781. (e) Mravik, A.; Böcskel, Z.; Katona, Z.; Markovits, I.; Fogassy, E. *Angew. Chem., Int. Ed. Engl.* **1997**, *36*, 1534.

(8) Taylor, R.; Kennard, O.; Versichel, W. *J. Am. Chem. Soc.* **1984**, *106*, 244.

(9) Umezawa, Y.; Tsuboyama, S.; Honda, K.; Uzawa, J.; Nishio, M. *Bull. Chem. Soc. Jpn.* **1998**, *71*, 1207 and references therein.

Table 1. Enantiomeric Recognition of α -Hydroxy Esters **2** by (R,R) -**1**


entry	Racemic 2			Optical Resolution			
	R ¹	R ²		guest/host ^a	% ee	config	sheet type
1	Me	Me	2a	1.00	89 ^b	<i>S</i>	folded
2	Me	Et	2b	1.00	97 ^c	<i>S</i>	folded
3	Me	<i>n</i> -Pr	2c	not included			
4	Me	<i>i</i> -Pr	2d	not included			
5	Et	Me	2e	1.00 (0.00, 0.28)	87 ^d	<i>S</i>	unknown
6	-C(CH ₃) ₂ CH ₂ -	Me	2f	0.50 (1.00, 0.36)	92 ^d	<i>S</i>	folded
7	<i>n</i> -Pr	Me	2g	0.53 (1.09, 0.00)	89 ^d	<i>S</i>	folded
8	<i>n</i> -Bu	Me	2h	0.50 (1.05, 0.00)	>99 ^d	<i>S</i>	folded
9	<i>i</i> -Bu	Me	2i	0.52 (1.10, 0.00)	87 ^d	<i>S</i>	folded
10	Ph	Me	2j	not included			
11			(S)-2j	0.50 (0.00, 1.00)			folded
12	<i>i</i> -Pr	Me	2k	0.50 (1.00, 0.50)	6 ^d	<i>R</i>	extended
13			(S)-2k	1.01			folded
14	<i>t</i> -Bu	Me	2l	0.50 (0.70, 0.50)	82 ^d	<i>S</i>	extended

^a Determined by ¹H NMR and elemental analysis. The ratios of methanol and water, respectively, in the inclusion compound are shown in parentheses. ^b Determined by chiral HPLC analysis (Chiralpak AS) after the benzylation of the hydroxyl group. ^c Determined by optical rotation after the benzylation of the hydroxy group. ^d Determined by chiral HPLC analysis (Chiralcel OD).

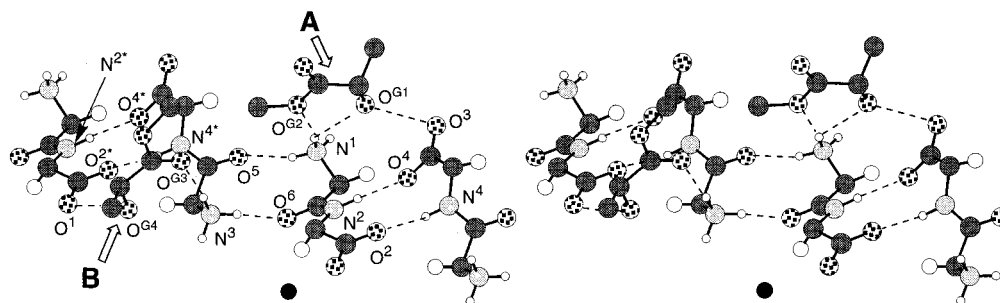


Figure 3. Hydrogen-bonding networks between (R,R) -**1** and (S) -**2a** (stereoview). The naphthyl and phenyl groups of (R,R) -**1** and hydrogen atoms of (S) -**2a** are omitted for clarity.

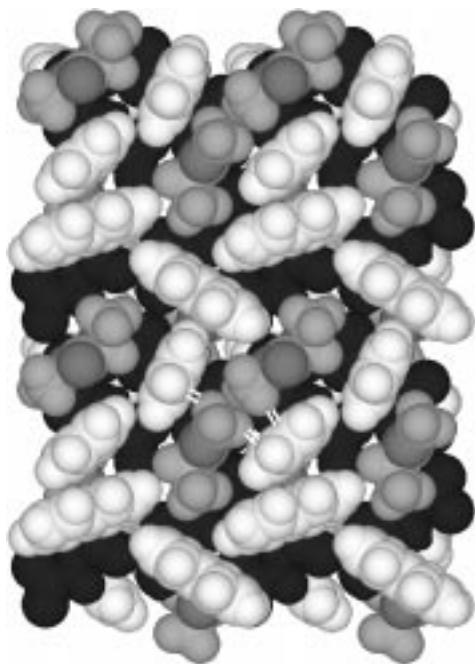


Figure 4. CPK model of packing in the inclusion compound of (R,R) -**1** and (S) -**2a** (the *a-c* plane). The naphthyl and phenyl groups of (R,R) -**1** and (S) -**2a** are colored white and gray, respectively. White double lines would be CH/π interaction between (R,R) -**1** and (S) -**2a**.

To obtain single crystals for the inclusion compounds, cocrystallization of (R,R) -**1** was performed with the chiral α -hydroxy esters, which are easily prepared from the corresponding chiral amino acids.¹⁰ We obtained the single crystals suitable for X-ray crystallography for (S) -**2b**, (S) -**2f**, (S) -**2g**, (S) -**2h**, and (S) -**2i**. The crystallographic data are summarized in Table 2. In these cases, (R,R) -**1** molecules are also arranged in the "folded antiparallel" mode that is similar to the case of (R,R) -**1**· (S) -**2a**. Superimposed representation of six "folded antiparallel" sheets showed that the dipeptide backbones are arranged in a fairly similar manner (Figure 5). These inclusion crystals having chiral pocket-type cavities are isostructural with an (R,R) -**1**· (S) -**2a** complex, and the stereochemistry of the included α -hydroxy esters is also the *S* form (Figure 6 a–e). Allylic alcohols, as achiral guest molecules, are also included in the same cavities (Figure 6f).⁶

In the case that the guest molecule is relatively large like **2f**, **2g**, **2h**, or **2i**, only one molecule of the guest was included in half of the cavity and the other half was occupied by some solvent molecules. This is because the two molecules are too large to be included in one cavity at the same time (Figure 6b–e). It is worth noting that the shape of the pocket cavity is scarcely changed,

(10) (a) Adam, W.; Fell, R. T.; Hoch, U.; Saha-Möller, C. R.; Schreier, P. *Tetrahedron: Asymmetry* **1995**, *6*, 1047. (b) Li, W.-R.; Ewing, W. R.; Harris, B. D.; Joullié, M. M. *J. Org. Chem.* **1990**, *55*, 7659.

Table 2. Crystallographic Data for Inclusion Compounds

	(R,R)-1-(S)-2a	(R,R)-1-(S)-2b	(R,R)-1-(S)-2f·MeOH·H ₂ O	(R,R)-1-(S)-2g·MeOH	(R,R)-1-(S)-2h·MeOH
mol formula	2C ₂₀ H ₁₈ O ₃ N ₂ ·2C ₄ H ₈ O ₃	2C ₂₀ H ₁₈ O ₃ N ₂ ·2C ₃ H ₁₀ O ₃	2C ₂₀ H ₁₈ O ₃ N ₂ ·C ₆ H ₁₀ O ₃ ·2CH ₄ O·H ₂ O	2C ₂₀ H ₁₈ O ₃ N ₂ ·C ₆ H ₁₀ O ₃ ·2CH ₄ O	2C ₂₀ H ₁₈ O ₃ N ₂ ·C ₇ H ₁₄ O ₃ ·2CH ₄ O
M _w	876.96	905.01	880.99	864.99	879.02
crystal system	orthorhombic	monoclinic	monoclinic	orthorhombic	orthorhombic
space group	P2 ₁ 2 ₁ 2 ₁	P2 ₁	P2 ₁	P2 ₁ 2 ₁ 2 ₁	P2 ₁ 2 ₁ 2 ₁
Z	4	2	2	4	4
a/Å	15.892(4)	13.647(3)	12.824(2)	16.102(6)	16.147(3)
b/Å	25.591(6)	15.905(3)	16.284(4)	24.925(6)	25.156(6)
c/Å	11.322(3)	11.468(3)	11.375(2)	11.389(2)	11.366(3)
β/deg	90.00	104.606(18)	106.31(1)	90.00	90.00
V/Å ³	4605(2)	2408.6(9)	2279.7(8)	4571(2)	4617(2)
D _{calc} /g cm ⁻³	1.265	1.248	1.283	1.257	1.265
T/K	298	298	173	173	173
total reflctns meas	5052	5155	4846	5010	5052
unique reflctns	4869	4737	4488	4338	4374
cutoff	3.00	3.00	3.00	3.00	3.00
Δρ _{max} /e Å ⁻³	0.19	0.26	1.43	0.32	0.33
Δρ _{min} /e Å ⁻³	-0.21	-0.24	-0.46	-0.31	-0.36
R	0.0503	0.0683	0.059	0.051	0.049
R _w	0.0487	0.0742	0.069	0.051	0.050
	(R,R)-1-(S)-2a	(R,R)-1-(S)-2b	(R,R)-1-(S)-2j·H ₂ O	(R,R)-1-(S)-2k	(R,R)-1-(S)-2l·MeOH·H ₂ O
mol formula	2C ₂₀ H ₁₈ O ₃ N ₂ ·C ₇ H ₁₄ O ₃ ·2CH ₄ O	2C ₂₀ H ₁₈ O ₃ N ₂ ·C ₉ H ₁₀ O ₃ ·2H ₂ O	2C ₂₀ H ₁₈ O ₃ N ₂ ·C ₆ H ₁₀ O ₃	2C ₂₀ H ₁₈ O ₃ N ₂ ·C ₆ H ₁₂ O ₃	2C ₂₀ H ₁₈ O ₃ N ₂ ·C ₇ H ₁₄ O ₃ ·2CH ₄ O·H ₂ O
M _w	879.02	870.96	870.96	933.07	897.04
crystal system	orthorhombic	orthorhombic	orthorhombic	monoclinic	orthorhombic
space group	P2 ₁ 2 ₁ 2 ₁	P2 ₁ 2 ₁ 2 ₁	P2 ₁ 2 ₁ 2 ₁	P2 ₁	P2 ₁ 2 ₁ 2 ₁
Z	4	4	4	2	4
a/Å	16.167(5)	16.124(4)	16.124(4)	13.329(3)	18.168(4)
b/Å	25.186(7)	25.193(6)	25.193(6)	16.176(4)	27.545(6)
c/Å	11.453(4)	11.441(4)	11.441(4)	11.513(3)	9.478(2)
β/deg	90.00	90.00	90.00	103.40(2)	90.00
V/Å ³	4663(2)	4647(2)	4647(2)	2415(1)	4743(2)
D _{calc} /g cm ⁻³	1.252	1.245	1.245	1.283	1.256
T/K	173	298	298	298	173
total reflctns meas	5092	5073	5073	5157	5226
unique reflctns	4409	4891	4891	4750	4510
cutoff	2.00	3.00	3.00	3.00	3.00
Δρ _{max} /e Å ⁻³	0.20	0.51	0.51	0.22	0.20
Δρ _{min} /e Å ⁻³	-0.21	-0.32	-0.32	-0.22	-0.21
R	0.065	0.0678	0.0678	0.0534	0.048
R _w	0.056	0.0782	0.0782	0.0583	0.050

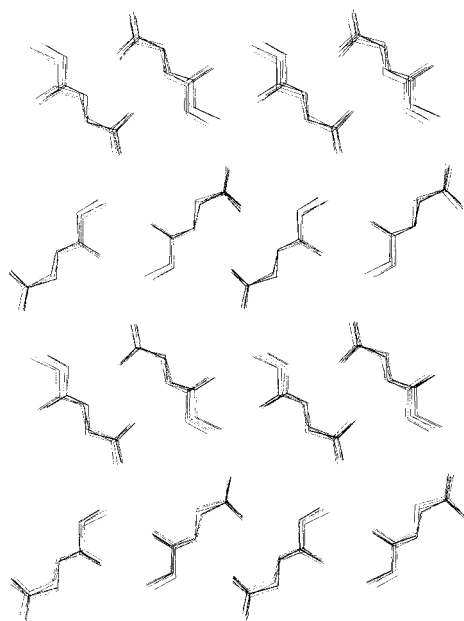


Figure 5. Superimposed representation of folded antiparallel arrangements of dipeptide backbones for such guest molecules as (*S*)-**2a**, (*S*)-**2b**, (*S*)-**2f**, (*S*)-**2g**, (*S*)-**2h**, and (*S*)-**2i**.

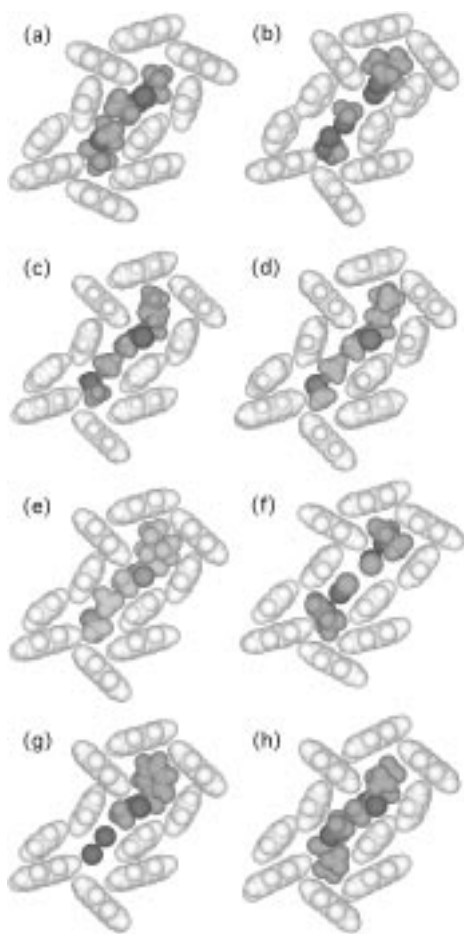


Figure 6. Comparison of chiral pocket-type cavities for various guest molecules: (a) (*R,R*)-**1**·(*S*)-**2b** (1:1), (b) (*R,R*)-**1**·(*S*)-**2f**·MeOH·H₂O (2:1:2:1), (c) (*R,R*)-**1**·(*S*)-**2g**·MeOH (2:1:2), (d) (*R,R*)-**1**·(*S*)-**2h**·MeOH (2:1:2), (e) (*R,R*)-**1**·(*S*)-**2i**·MeOH (2:1:2), (f) (*R,R*)-**1**·methallyl alcohol·MeOH (1:1:1), (g) (*R,R*)-**1**·(*S*)-**2j**·H₂O (2:1:2), and (h) (*R,R*)-**1**·(*S*)-**2k** (1:1). The naphthyl and phenyl groups of (*R,R*)-**1** and guest molecules are colored white and gray, respectively.

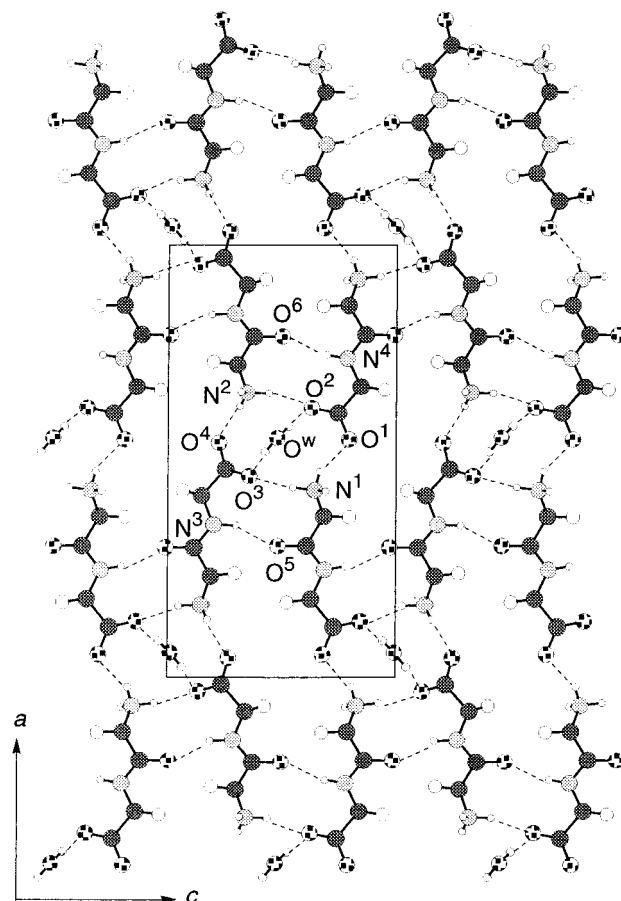


Figure 7. Sheet structure of dipeptide backbones of the inclusion compound (*R,R*)-**1**·(*S*)-**2l** (the *a*-*c* plane). The naphthyl and phenyl groups of (*R,R*)-**1**, (*S*)-**2l**, and methanols are omitted for clarity. A unit cell is shown using a box.

independent of the shape of the guest molecule. We tried to crystallize (*R,R*)-**1** with racemic methyl mandelate **2j** or its *R* enantiomer, but the guest molecules were not included to give rise to the formation of the (*R,R*)-**1**·methanol crystals. Nevertheless, optically pure (*S*)-**2j** afforded an inclusion compound [(*R,R*)-**1**·(*S*)-**2j**·H₂O = 2:1:2] (entry 11 in Table 1), and (*S*)-**2j** was included with water molecules in the pocket-type cavity (Figure 6g). These results suggested that the presence of (*R*)-**2j** molecules prevents formation of the inclusion compound.

“Extended Antiparallel” Mode with the Channel-Type Cavity. When the guests are **2k** and **2l**, which have bulkier alkyl groups, another arrangement mode of (*R,R*)-**1** molecules was observed in the inclusion crystal (entries 12 and 14 in Table 1). Crystallographic data for the inclusion compound of (*R,R*)-**1**·(*S*)-**2l** are shown in Table 2. As shown in Figure 7, in this crystal, the salt formation between the amino and carboxyl groups of (*R,R*)-**1** contributes to the linkage of the dipeptide molecules (N¹···O¹, N¹···O³, N²···O², and N²···O⁴, 2.66, 2.85, 2.83, and 2.67 Å, respectively) to form a ribbon structure along the *a* axis. Two amino groups and two carboxyl groups formed a 12-membered hydrogen-bonded ring,¹¹ and a water molecule was bridged by the hydrogen-bonding between two carboxyl groups (O²···O^w and O³···O^w, 2.69 and 2.73 Å, respectively). The central amide proton of (*R,R*)-**1** is bound to the amide oxygen of the neighboring (*R,R*)-**1** molecules with 2.87 (N³···O⁵) and 2.90 (N⁴···O⁶) Å to construct the linkage along the *c* axis. Thus, (*R,R*)-**1** molecules were arranged in an antiparallel

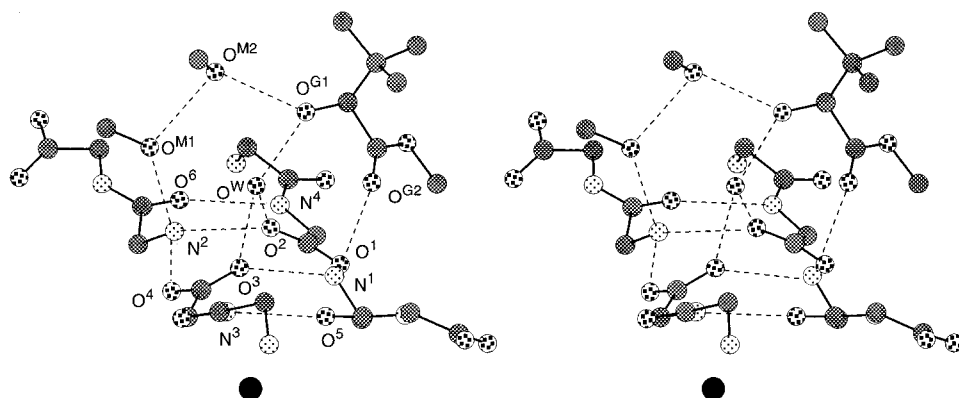


Figure 8. Hydrogen-bonding networks between (*R,R*)-**1** and (*S*)-**21**, methanol, and water (stereoview). The naphthyl and phenyl groups of (*R,R*)-**1** and hydrogen atoms are omitted for clarity.

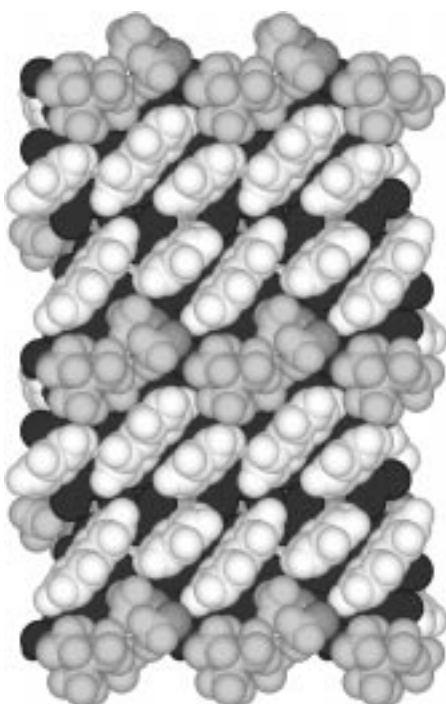


Figure 9. CPK model of packing in the inclusion compound of (*R,R*)-**1** and (*S*)-**21** (the *a-c* plane). The naphthyl and phenyl groups of (*R,R*)-**1** and guest molecules are colored white and gray, respectively.

mode. We call this mode “extended antiparallel” (Figure 1c). Figure 8 depicts the arrangement of the guest molecules on the dipeptide sheet and the crucial interaction between (*R,R*)-**1** and the guest. The hydroxyl group of (*S*)-**21** is linked to one $^+\text{NH}_3$ of (*R,R*)-**1** through hydroxyl groups of two methanol molecules ($\text{N}^2 \cdots \text{O}^{\text{M}1}$, $\text{O}^{\text{M}1} \cdots \text{O}^{\text{M}2}$, and $\text{O}^{\text{M}2} \cdots \text{O}^{\text{G}1}$, 2.83, 2.94, and 2.82 Å, respectively), and it also interacts with two carboxyl oxygens of (*R,R*)-**1** through one water molecule ($\text{O}^{\text{W}} \cdots \text{O}^{\text{G}1}$, 2.65 Å). The carbonyl oxygen ($\text{O}^{\text{G}2}$) of (*S*)-**21** was connected to another $^+\text{NH}_3$ of (*R,R*)-**1** ($\text{N}^1 \cdots \text{O}^{\text{G}2}$, 2.89 Å). So, the included methanols and (*S*)-**21** make a bridge between two neighboring ribbon structures of (*R,R*)-**1**.

(11) Hydrogen bonding of the 12-membered ring structure is also observed in several ammonium carboxylates. For recent papers, see: (a) Akazome, M.; Takahashi, T.; Ogura, K. *Tetrahedron Lett.* **1998**, 39, 4839. (b) Kinbara, K.; Kai, A.; Maekawa, Y.; Hashimoto, Y.; Naruse, S.; Hasegawa, M.; Saigo, K. *J. Chem. Soc., Perkin Trans. 2* **1996**, 247. (c) Kozma, D.; Böcskei, Z.; Simon, K.; Fogassy, E. *J. Chem. Soc., Perkin Trans. 2* **1994**, 1883.

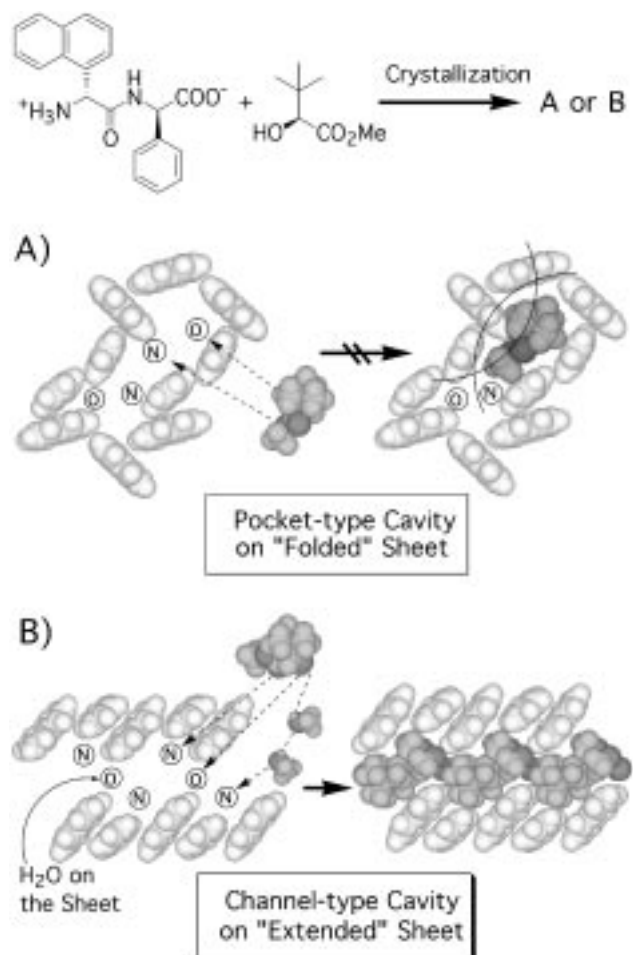


Figure 10. Illustration of optional formation of the “extended” antiparallel sheet. Trial inclusion into each types of cavities using (*S*)-**21** as the guest molecule. (A) A pocket-type cavity on the folded sheet. (B) A channel-type cavity on the extended sheet.

Figure 9 shows a top view of the CPK model from the *a-c* plane of the inclusion compound of (*S*)-**21**·MeOH·H₂O. The guest molecules were included in a one-dimensional channel having the walls of the stacking naphthyl and phenyl groups. The stacking mode of the naphthyl and phenyl groups is “parallel stacked and displaced”, which has been already found in the case of the inclusion compound of (*R*)-phenylglycyl-(*R*)-phenylglycine with a disulfoxide.¹² Figure 10 illustrates the reason the “extended antiparallel” sheet is formed in the

case of (*S*)-**2l**: (*S*)-**2l** could not be included in this pocket-type cavity because the bulky *tert*-butyl group of (*S*)-**2l** suffers from the steric repulsion of the walls of this chiral cavity. As a result, the conformation and arrangement of the dipeptide are compelled to be the "extended" antiparallel mode with a channel cavity. In other words, the channel-type cavity may be too loose to include relatively small guest molecules. If the guest molecule is small, the arrangement of (*R,R*)-**1** molecules would shrink to be the "folded antiparallel" mode with a chiral pocket-type cavity and to gain sufficient packing and/or host-guest interactions.

Interestingly, the same extended antiparallel mode with the channel-type cavity was observed in the case that racemic **2k** was included. This is in contrast with the pocket-type inclusion of (*S*)-**2k** in the "folded antiparallel" mode (entry 13 in Table 1 and Figure 6h). By single-crystal X-ray analysis of the inclusion compound of racemic **2k**, the arrangement of dipeptide (*R,R*)-**1** was confirmed, but the hydroxy ester could not be identified because of the disorder of guest molecules and/or the contamination of the opposite enantiomer.¹³ This result supported that **2k** was not recognized stereoselectively in the chiral cavity of (*R,R*)-**1** (entry 12 in Table 1).

Concluding Remarks

We found that a simple dipeptide, (*R,R*)-**1**, included α -hydroxy esters to construct two kinds of "antiparallel" β -sheetlike structures, namely, "folded" or "extended" mode. In both cases, α -hydroxy esters were captured stereoselectively by multiple hydrogen bonding in the void between the layers of (*R,R*)-**1**, and the stereochemistry of the included α -hydroxy esters was predominantly the *S* form. When the guest α -hydroxy esters are relatively small, (*R,R*)-**1** molecules arrange in the "folded antiparallel" mode to form a sheet of (*R,R*)-**1** and chiral pocket-type cavities surrounded by aryl groups. Larger α -hydroxy esters with a bulky alkyl group like (*S*)-**2l** were not included in the pocket cavity. As a result, the dipeptide molecules arrange in "extended antiparallel" mode to include the bulky guest molecules. Consequently, the arrangement of (*R,R*)-**1** molecules is governed by the size or shape of α -hydroxy esters to form optional sheet structures with adjustable cavities for highly enantiomeric inclusion of the α -hydroxy ester.

Experimental Section

Decomposition points of the inclusion compounds were uncorrected. Elemental analyses were performed at Chemical Analysis Center, Chiba University, Japan. (*R*)-(1-Naphthyl)glycyl-(*R*)-phenylglycine was prepared according to our previous literature.⁵

Preparation for α -Hydroxy Esters.¹⁰ (*S*)- α -Amino acid (30 mmol) was suspended in water (22 mL) at 0 °C, and 1 M H₂SO₄ (16.5 mL) was added dropwise with stirring. After the (*S*)- α -amino acid was dissolved, 2 M NaNO₂ (16.5 mL) was added dropwise, and the rate of addition of the acid was adjusted similarly. After the addition was complete, the solution was stirred at 0 °C for 3 h and then allowed to stir at room temperature for 12 h. Then, the reaction mixture was

extracted with ethyl acetate (50 mL \times 4), dried on anhydrous MgSO₄, filtered, and concentrated in vacuo. The resulting crude solid was recrystallized from ether/petroleum ether at 0 °C to afford (*S*)- α -hydroxy acid (50–70% yield) as a colorless crystal. Concentrated H₂SO₄ (0.1 mL) was added to a solution of (*S*)- α -hydroxy acid (10 mmol) in MeOH (50 mL) and refluxed for 3 h. The reaction was concentrated in vacuo, diluted with ether (200 mL), and washed with saturated NaHCO₃ (30 mL \times 3) and brine (30 mL \times 1). The organic layer was dried on anhydrous MgSO₄, filtered, and concentrated. The crude oil was then distilled in vacuo to afford (*S*)- α -hydroxy acid methyl ester (75–90% yield) as a colorless oil. Racemic α -hydroxy esters are prepared in a similar manner as above.

Preparation of Inclusion Compounds. To a solution of (*R*)-(1-naphthyl)glycyl-(*R*)-phenylglycine (0.10 mmol) in methanol (0.35 mL) was added hydroxy ester (0.20 mmol, 2 mol equiv) at room temperature. After several days, the precipitated crystals were filtrated, washed with chloroform (3 mL), and dried in vacuo to afford the inclusion compound of (*R*)-(1-naphthyl)glycyl-(*R*)-phenylglycine- α -hydroxy ester. The inclusion compound was dissolved in water (5 mL), and an extraction with ether (10 mL \times 3) was performed. The combined organic layers were dried with anhydrous MgSO₄, and concentrated under reduced pressure. The crude oil was then distilled in vacuo to afford hydroxy ester as a colorless oil. Enantiomeric excess of hydroxy ester was detected by optical rotation or chiral HPLC after benzylation of hydroxy group, if necessary (Daicel Chiralcel OD or Chiralpak AS). Absolute configurations were determined by single-crystal X-ray analysis of inclusion compounds (method A), comparison with authentic samples of (*S*)- α -hydroxy esters synthesized from (*S*)- α -amino acid (method B), or optical rotations (method C).

Benzoylated **2a:** eluent, hexane/2-propanol (9:1); flow rate, 0.7 mL/min, $t_R(R)$ = 12.5 min, $t_R(S)$ = 15.8 min (Daicel Chiralpak AS). The absolute configuration was determined by methods A and B.

Benzoylated **2b:** $[\alpha]^{25}_D = +18.00$ (*c* 1.45, CHCl₃) (lit.^{14a} (*S*)-(+)-**2b** $[\alpha]^{21}_D = +18.35$ (*c* 2.46, CHCl₃)). The absolute configuration was determined by methods A and C.

2e: eluent, hexane/2-propanol (30:1); flow rate, 0.5 mL/min, $t_R(S)$ = 15.1 min, $t_R(R)$ = 16.7 min (Daicel Chiralcel OD). The absolute configuration was determined by method B.^{10a}

2f: eluent, hexane/2-propanol (30:1); flow rate, 0.8 mL/min, $t_R(R)$ = 29.0 min, $t_R(S)$ = 33.4 min (Daicel Chiralcel OD). The absolute configuration was determined by methods A and C (lit.^{14b} (*R*)-(-)-**2f** $[\alpha]^{25}_D = -50.7$ (*c* 2.05, H₂O)).

2g: eluent, hexane/2-propanol (30:1); flow rate, 0.5 mL/min, $t_R(S)$ = 15.1 min, $t_R(R)$ = 18.0 min (Daicel Chiralcel OD). The absolute configuration was determined by method A.

2h: eluent, hexane/2-propanol (30:1); flow rate, 0.4 mL/min, $t_R(S)$ = 18.0 min, $t_R(R)$ = 20.2 min (Daicel Chiralcel OD). The absolute configuration was determined by method A.

2i: eluent, hexane/2-propanol (30:1); flow rate, 0.3 mL/min, $t_R(S)$ = 25.1 min, $t_R(R)$ = 28.1 min (Daicel Chiralcel OD). The absolute configuration was determined by methods A and B.

2k: eluent, hexane/2-propanol (30:1); flow rate, 0.5 mL/min, $t_R(S)$ = 12.7 min, $t_R(R)$ = 14.8 min (Daicel Chiralcel OD). The absolute configuration was determined by method B.^{10b}

2l: eluent, hexane/2-propanol (30:1); flow rate, 0.5 mL/min, $t_R(S)$ = 11.2 min, $t_R(R)$ = 12.7 min (Daicel Chiralcel OD). The absolute configuration was determined by methods A and B.

Inclusion compound of (*R*)-(1-naphthyl)glycyl-(*R*)-phenylglycine-methyl lactate [(*R,R*)-1-2a**] complex:** 56% yield based on dipeptide; colorless solid; dec 146–147 °C (sintering); ¹H NMR (D₂O, 300 MHz) δ 8.13–8.04 (m, 3H), 7.75–7.59 (m, 4H), 7.42–7.27 (d like, 5H), 5.96 (s, 1H), 5.19 (s, 1H), 4.40 (q, *J* = 7.01 Hz, 1.00H), 3.75 (s, 2.98H), 1.39 (d, *J* = 7.01 Hz, 2.99H); IR (KBr) 3281, 3222, 1744, 1735, 1671, 1595 cm⁻¹. Anal. Calcd for C₂₀H₁₈N₂O₃·1.00C₄H₈O₃: C, 65.74; H, 5.98; N, 6.39. Found: C, 65.44; H, 5.90; N, 6.59.

(12) Akazome, M.; Noguchi, M.; Tanaka, O.; Sumikawa, A.; Uchida, T.; Ogura, K. *Tetrahedron* **1997**, *53*, 8315.

(13) Crystal data for (*R,R*)-**1**-racemic **2k**·MeOH·H₂O: 2C₂₀H₁₈O₃N₂·C₆H₁₂O₃·2CH₄O·H₂O, *M_w* 883.01, orthorhombic, *P*2₁2₁2₁ with *a* = 18.203(4) Å, *b* = 27.185(7) Å, *c* = 9.512(2) Å, *V* = 4707(2) Å³, *Z* = 4, *D_{cal}* = 1.246 g cm⁻³, temperature of data collection, 173 K; *R* ~ 0.12.

(14) (a) Cohen, S. G.; Weinstein, S. Y. *J. Am. Chem. Soc.* **1964**, *86*, 5326. (b) Stillier, E. T.; Harris, S. A.; Finkelstein, J.; Keresztesy, J. C.; Folkers, K. *J. Am. Chem. Soc.* **1940**, *62*, 1785.

Inclusion compound of (*R*)-(1-naphthyl)glycyl-(*R*)-phenylglycine-ethyl lactate [(*R,R*)-1-2b] complex: 75% yield based on dipeptide; colorless solid; dec 141.5–143 °C (sintering); ¹H NMR (D₂O, 300 MHz) δ 8.14–8.05 (m, 3H), 7.75–7.59 (m, 4H), 7.42–7.30 (d like, 5H), 5.98 (s, 1H), 5.18 (s, 1H), 4.37 (q, *J* = 7.01 Hz, 1.00H), 4.20 (q, *J* = 7.14 Hz, 2.00H), 1.39 (d, *J* = 7.01 Hz, 3.00H), 1.11 (t, *J* = 7.14 Hz, 3.00H); IR (KBr) 3269, 3219, 1741, 1722, 1671, 1595 cm⁻¹. Anal. Calcd for C₂₀H₁₈N₂O₃ · 1.00C₅H₁₀O₃: C, 66.36; H, 6.24; N, 6.19. Found: C, 66.22; H, 6.23; N, 6.32.

Inclusion compound of (*R*)-(1-naphthyl)glycyl-(*R*)-phenylglycine-methyl 2-hydroxybutyrate·H₂O [(*R,R*)-1-2e·H₂O] complex: 75% yield based on dipeptide; colorless solid; dec 142–143 °C (sintering); ¹H NMR (D₂O, 300 MHz) δ 8.14–8.05 (m, 3H), 7.75–7.60 (m, 4H), 7.42–7.30 (d like, 5H), 5.97 (s, 1H), 5.17 (s, 1H), 4.27 (t like, 1.00H), 3.75 (s, 3.00H), 1.87–1.63 (m, 2.00H), 0.91 (t, *J* = 7.14 Hz, 3.00H); IR (KBr) 3275, 3222, 1751, 1726, 1670, 1592 cm⁻¹. Anal. Calcd for C₂₀H₁₈N₂O₃ · 1.00C₅H₁₀O₃ · 0.28H₂O: C, 65.62; H, 6.29; N, 6.12. Found: C, 65.61; H, 6.17; N, 6.24.

Inclusion compound of (*R*)-(1-naphthyl)glycyl-(*R*)-phenylglycine-pantolactone-methanol·H₂O [(*R,R*)-1-2f·MeOH·H₂O] complex: 82% yield based on dipeptide; colorless unstable solid; ¹H NMR (D₂O, 300 MHz) δ 8.15–8.05 (m, 3H), 7.78–7.62 (m, 4H), 7.43–7.32 (d like, 5H), 5.98 (s, 1H), 5.19 (s, 1H), 4.37 (s, 0.50H), 4.11 (ABq, *J* = 8.99 Hz, 1.00H), 3.35 (s, 3.00H), 1.18 (s, 1.50H), 1.01 (s, 1.50H); IR (KBr) 3371, 3253, 1774, 1668, 1600 cm⁻¹. Anal. Calcd for C₂₀H₁₈N₂O₃ · 0.50C₆H₁₀O₃ · 1.00CH₄O · 0.36H₂O: C, 65.82; H, 6.38; N, 6.40. Found: C, 65.84; H, 6.35; N, 6.32.

Inclusion compound of (*R*)-(1-naphthyl)glycyl-(*R*)-phenylglycine-methyl 2-hydroxyvalerate-methanol [(*R,R*)-1-2g·MeOH] complex: 77% yield based on dipeptide; colorless solid; dec 120–122 °C; ¹H NMR (D₂O, 300 MHz) δ 8.15–8.05 (m, 3H), 7.78–7.62 (m, 4H), 7.43–7.32 (d like, 5H), 5.98 (s, 1H), 5.19 (s, 1H), 4.40–4.30 (t like, 0.53H), 3.75 (s, 1.59H), 3.34 (s, 3.27H), 1.83–1.60 (m, 1.06H), 1.44–1.25 (m, 1.06H), 0.91 (t, *J* = 7.4 Hz, 1.59H); IR (KBr) 3246, 1741, 1670, 1595 cm⁻¹. Anal. Calcd for C₂₀H₁₈N₂O₃ · 0.53C₆H₁₂O₃ · 1.09CH₄O: C, 66.35; H, 6.59; N, 6.38. Found: C, 66.04; H, 6.42; N, 6.67.

Inclusion compound of (*R*)-(1-naphthyl)glycyl-(*R*)-phenylglycine-methyl 2-hydroxyhexanoate-methanol [(*R,R*)-1-2h·MeOH] complex: 67% yield based on dipeptide; colorless solid; dec 98–99 °C; ¹H NMR (D₂O, 300 MHz) δ 8.15–8.05 (m, 3H), 7.78–7.62 (m, 4H), 7.43–7.32 (d like, 5H), 5.98 (s, 1H), 5.19 (s, 1H), 4.40–4.30 (t like, 0.50H), 3.75 (s, 1.50H), 3.34 (s, 3.15H), 1.83–1.60 (m, 1.00H), 1.42–1.22 (m, 2.00H), 0.91 (t, *J* = 7.1 Hz, 1.50H); IR (KBr) 3242, 1741, 1670, 1584 cm⁻¹. Anal. Calcd for C₂₀H₁₈N₂O₃ · 0.50C₇H₁₄O₃ · 1.05CH₄O: C, 66.85; H, 6.67; N, 6.35. Found: C, 66.55; H, 6.39; N, 6.54.

Inclusion compound of (*R*)-(1-naphthyl)glycyl-(*R*)-phenylglycine-methyl 2-hydroxy-4-methylvalerate-methanol [(*R,R*)-1-2i·MeOH] complex: 80% yield based on dipeptide; colorless solid; dec 95–96.5 °C; ¹H NMR (D₂O, 300 MHz) δ 8.15–8.05 (m, 3H), 7.78–7.62 (m, 4H), 7.43–7.32 (d like, 5H), 5.98 (s, 1H), 5.19 (s, 1H), 4.50–4.37 (t like, 0.52H), 3.75 (s, 1.56H), 3.34 (s, 3.30H), 1.83–1.60 (m, 0.52H), 1.63–1.53 (m, 1.04H), 0.92 (d, *J* = 6.5 Hz, 3.12H); IR (KBr) 3349, 3255, 1735, 1671, 1584 cm⁻¹. Anal. Calcd for C₂₀H₁₈N₂O₃ · 0.52C₇H₁₄O₃ · 1.10CH₄O: C, 66.68; H, 6.71; N, 6.29. Found: C, 66.39; H, 6.59; N, 6.50.

Inclusion compound of (*R*)-(1-naphthyl)glycyl-(*R*)-phenylglycine-(*S*)-methyl mandelate·H₂O [(*R,R*)-1-(*S*)-2j·H₂O] complex: 47% yield based on dipeptide; colorless solid;

dec 109.5–110.5 °C; ¹H NMR (D₂O, 300 MHz) δ 8.14–8.05 (m, 3H), 7.75–7.59 (m, 4H), 7.42–7.27 (m, 7.50H), 5.96 (s, 1H), 5.35 (s, 0.50H), 5.17 (s, 1H), 3.71 (s, 1.50H); IR (KBr) 3255, 1743, 1671, 1597 cm⁻¹. Anal. Calcd for C₂₀H₁₈N₂O₃ · 0.50C₉H₁₀O₃ · 1.00H₂O: C, 67.57; H, 5.79; N, 6.43. Found: C, 67.47; H, 5.96; N, 6.18.

Inclusion compound of (*R*)-(1-naphthyl)glycyl-(*R*)-phenylglycine-methyl 2-hydroxy-3-methylbutyrate-methanol·H₂O [(*R,R*)-1-2k·MeOH·H₂O] complex: 81% yield based on dipeptide; colorless solid; dec 126–127 °C; ¹H NMR (D₂O, 300 MHz) δ 8.15–8.07 (m, 3H), 7.77–7.62 (m, 4H), 7.44–7.33 (d like, 5H), 5.98 (s, 1H), 5.19 (s, 1H), 4.16 (d, *J* = 4.53 Hz, 0.50H), 3.78 (s, 1.50H), 3.38 (s, 3.00H), 2.13–2.04 (m, 0.50H), 0.97 (d, *J* = 6.87 Hz, 1.50H), 0.88 (d, *J* = 6.87 Hz, 1.50H); IR (KBr) 3297, 1725, 1655, 1604 cm⁻¹. Anal. Calcd for C₂₀H₁₈N₂O₃ · 0.50C₆H₁₂O₃ · 1.00CH₄O · 0.50H₂O: C, 65.29; H, 6.62; N, 6.35. Found: C, 65.56; H, 6.43; N, 6.37.

Inclusion compound of (*R*)-(1-naphthyl)glycyl-(*R*)-phenylglycine-(*S*)-methyl 2-hydroxy-3-methylbutyrate [(*R,R*)-1-(*S*)-2k] complex: 38% yield based on dipeptide; colorless solid; dec 139.5–140.5 °C (sintering); ¹H NMR (D₂O, 300 MHz) δ 8.15–8.07 (m, 3H), 7.77–7.62 (m, 4H), 7.44–7.33 (d like, 5H), 5.98 (s, 1H), 5.19 (s, 1H), 4.16 (d, *J* = 4.53 Hz, 1.01H), 3.78 (s, 3.03H), 2.13–2.04 (m, 1.01H), 0.97 (d, *J* = 6.87 Hz, 3.03H), 0.88 (d, *J* = 6.87 Hz, 3.03H); IR (KBr) 3262, 3222, 1751, 1724, 1669, 1591 cm⁻¹. Anal. Calcd for C₂₀H₁₈N₂O₃ · 1.01C₆H₁₂O₃: C, 66.90; H, 6.49; N, 5.99. Found: C, 66.63; H, 6.26; N, 6.21.

Inclusion compound of (*R*)-(1-naphthyl)glycyl-(*R*)-phenylglycine-methyl 3,3-dimethyl-2-hydroxybutyrate-methanol·H₂O [(*R,R*)-1-2l·MeOH·H₂O] complex: 83% yield based on dipeptide; colorless unstable solid; ¹H NMR (D₂O, 300 MHz) δ 8.14–8.05 (m, 3H), 7.76–7.61 (m, 4H), 7.42–7.33 (d like, 5H), 5.96 (s, 1H), 5.18 (s, 1H), 3.97 (s, 0.50H), 3.76 (s, 1.50H), 3.34 (s, 2.10H), 0.94 (s, 4.50H); IR (KBr) 3286, 1719, 1658, 1619 cm⁻¹. Anal. Calcd for C₂₀H₁₈N₂O₃ · 0.50C₇H₁₄O₃ · 0.70CH₄O · 0.50H₂O: C, 66.22; H, 6.61; N, 6.38. Found: C, 66.33; H, 6.60; N, 6.53.

X-ray Crystallography. Data collection was performed on a Mac Science MXC18 four-circle diffractometer with graphite-monochromated Cu Kα (*λ* = 1.541 78 Å) radiation using the 2θ-ω scan technique, and the X-ray intensities were measured up to 2θ = 140° at 298 or 173 K, respectively. The structures were solved and refined by a computer program package; CRYSTAN-GM ver. 6.2.1 or maXus ver. 1.1 from MAC Science Co. Ltd. The structures solved by a direct method (SIR 92¹⁵ on a computer program package).

Acknowledgment. This work was supported by "Research for the Future" Program (JSPS-RFTF96-P00304) from The Japan Society for the Promotion of Science.

Supporting Information Available: Tables of atomic coordinates and thermal parameters, bond lengths and angles, and ORTEP views of inclusion compounds of (*S*)-2a, (*S*)-2b, (*S*)-2f, (*S*)-2g, (*S*)-2h, (*S*)-2i, (*S*)-2j, racemic 2k, (*S*)-2k, and (*S*)-2l. This material is available free of charge via the Internet at <http://pubs.acs.org>.

JO9818778

(15) Altomare, A.; Cascarano, G.; Giacovazzo, C.; Guagliardi, A.; Burla, M. C.; Polidori, G.; Camalli, M. *J. Appl. Crystallogr.* **1994**, *27*, 435.